BIOCHEMISTRY
including biophysical chemistry & molecular biology

Article

pubs.acs.org/biochemistry

Nearly Reversible Conformational Change of Amyloid Fibrils as Revealed by pH-Jump Experiments

Kei-ichi Yamaguchi,[†,‡] Yuji O. Kamatari,[‡,§] Mayuko Fukuoka,[†,‡] Reiji Miyaji,[¶] and Kazuo Kuwata*[,†,‡]

[†]United Graduate School of Drug Discovery and Medical Information Sciences, [‡]Center for Emerging Infectious Diseases, [§]Life Science Research Center, and [¶]Supporting and Development Center for Technology Education, Faculty of Engineering, Gifu University, Yanagido 1-1, Gifu 501-1193, Japan

Supporting Information

ABSTRACT: pH-jump induced conformational transitions between substates of preformed amyloid fibrils made by a fragmented peptide of helix 2 (H2 peptide) of MoPrP were detected, and their kinetics were analyzed using a novel pH-jump apparatus specially designed for observing amyloids. Previously, we reported that H2 peptide formed ordered fibrils with a minimum at 207 nm on CD spectra at pH 2.9 (named pH 2.9 fibrils), but formed aggregate-like fibrils with a minimum at 220 nm at pH 7.5 (named pH 7.5 fibrils). When pH-jump from 2.9 to 7.5 was performed, the CD spectrum changed instantly, but the finally observed ellipticities were clearly distinct from those of pH 7.5 fibrils. Thus, the finally observed state is termed 'pH 7.5-like fibrils'. However, pH 7.5-like fibrils reverted to the conformation very similar to that of the pH 2.9 fibrils when the pH of the solution was restored to 2.9. Then, we examined the kinetics of the nearly reversible conformational changes between pH 2.9 fibrils and pH 7.5-like fibrils using ANS fluorescence stopped-flow, and we observed relatively fast phases (0.7−18 s^{-1}). In contrast, the conversion between pH 7.5-like fibrils and pH 7.5 fibrils never occurred (<0.2 day^{-1}). Thus, H2 fibrils can be switched readily between distinct conformations separated by a low energy barrier, while a large energy barrier clearly separated the different conformations. These conformational varieties of amyloid fibrils may explain the physical basis of the diversity in prion.

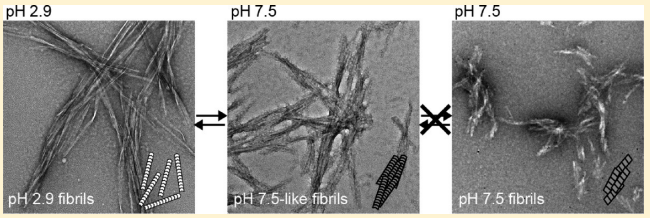

Amyloid fibrils may be associated with many neurodegenerative diseases such as Alzheimer's, Parkinson's, and prion diseases.[1−4] Prion diseases are a group of fatal neurodegenerative diseases, including Creutzfeldt-Jakob disease (CJD) and kuru in humans, as well as scrapie and bovine spongiform encephalopathy (BSE) in animals. Prion diseases emerged as a major public issue following epidemics of BSE, which crossed the species barrier to cause variant CJD in humans.[5,6] Pathogenesis of these unusual diseases is associated with the conformational rearrangement of a cellular isoform of prion protein (PrP^C) to a scrapie isoform (PrP^{Sc}) in the brain.[3,7,8] While PrP^C is monomeric and rich in α-helical structure,[9] the PrP^{Sc} conformer is characterized by an increased proportion of β-sheet structure and a propensity to aggregate into amyloid fibrils or plaques.[10]

The formation of multiple phenotypes of prion strains which are transmitted within the same or distinct species can be caused by the template-dependent polymerization reaction of PrP^{Sc}.[11−14] Mammalian prion amyloids from different species were shown to adopt distinct secondary structures and morphologies measured by Fourier transform infrared (FT-IR) and atomic force microscopy, respectively.[12] Importantly, cross-seeding of prion monomers from one species with preformed fibrils from another species produced a new amyloid strain that exhibits the secondary structure and morphology of the template fibrils.[12] Moreover, selective pressures result in the emergence of various mutants, and biologically cloned prion populations gradually become heterogeneous by accumulating mutants.[15] Prions may show the hallmarks of Darwinian evolution. Thus, conformational and morphological changes of amyloid fibrils formed from the same protein are one of the most intriguing aspects of amyloid studies,[16] because the fibril conformation, the fibril biological activity, and the toxicity might be correlated.

However, their high molecular weight and noncrystalline assembly preclude the use of conventional structural biological tools, such as X-ray crystallography or solution NMR, which are typically used for acquiring high-resolution structural information. Recently, it has been found that magic-angle-spinning solid-state NMR methods are suitable for use on amyloid fibrils, and can visualize atomic-level structure, in which β-strands are stacked in parallel and in register.[17−19] A report of the structure of a short amyloidogenic peptide, revealed by X-ray diffraction of a microcrystal, is consistent with this view.[20] In contrast, Knowles et al. reported that mature amyloid fibrils are stiffer than most functional intracellular biological filaments,[21] such as tubulin and actin filaments, and are stabilized mainly by an interbackbone hydrogen-bonding network and further modulated by variable side-chain interactions. Although conversion

Received: June 2, 2013
Revised: September 2, 2013
Published: September 3, 2013

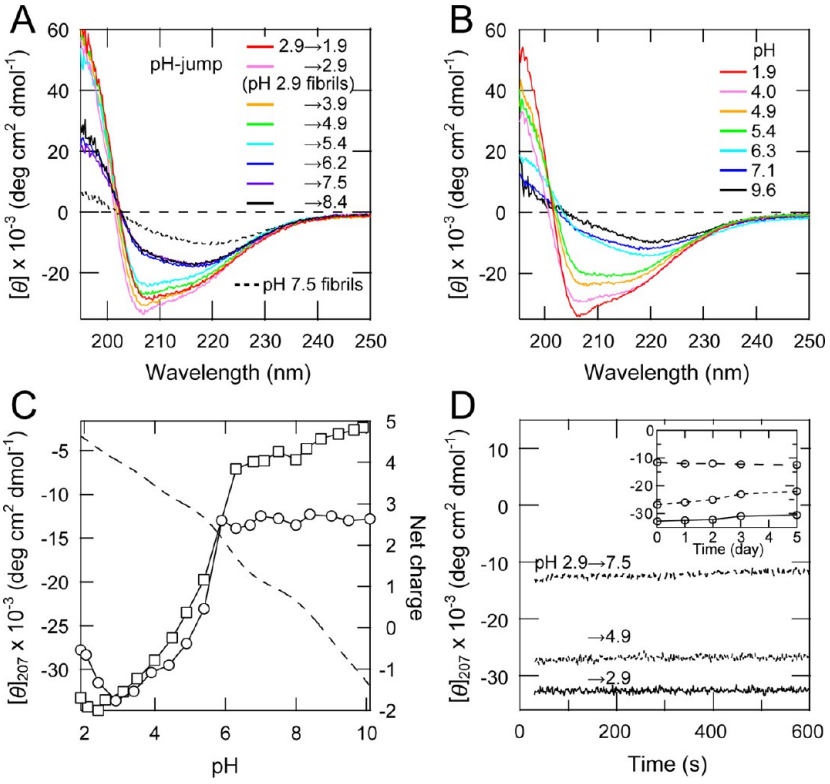

Figure 1. Single pH-jump experiments of H2 amyloid fibrils. (A) CD spectra of H2 fibrils after the pH-jump from 2.9 to various pH values (solid line) and that of pH 7.5 fibrils formed at pH 7.5 (dotted line). (B) CD spectra of H2 fibrils formed under various pH conditions after incubation for 2 days, taken from Yamaguchi et al.[26] (C) Conformational changes of H2 fibrils after the pH-jump from 2.9 to various pHs (○) and fibril formation of the H2 peptide under the various pH conditions (□) monitored as ellipticity at 207 nm. The net charge of the H2 peptide is indicated by a dashed line (right ordinate). (D) Conformational changes of H2 fibrils after a manual pH-jump, monitored as ellipticity at 207 nm with a dead time of 30 s. The inset shows the conformational changes of H2 fibrils after pH-jumps from 2.9 to 2.9 (solid line), 4.9 (dotted line), and 7.5 (dashed line) during incubation for 5 days at 25 °C.

from a native fold into the amyloid state is a complex process that involves several consecutive steps, including the initial formation of small oligomeric aggregates,[22,23] the conversion to the amyloid state represents the most conformationally rigid and thermodynamically stable folding.[2,21]

Previously, we reported that helix 2 region of mouse prion protein (MoPrP) (Figure S1 of the Supporting Information) was relatively hydrophobic and had a high propensity of β-sheet conformation among MoPrP, predicted by primary structure analyses using hydrophobicity scales[24] and ANTHEPROT,[25] respectively. We also reported a fragmented peptide of helix 2 (H2 peptide) formed ordered fibrils with a minimum in its circular dichroism (CD) spectrum at 207 nm at acidic pHs (Figure 1B), but aggregate-like fibrils with a minimum at 220 nm were formed at slightly basic pHs near the isotropic point (pI) of 8.6 (Figure 1B).[26] In addition, the recent studies indicate that the low pH solution is an ideal trigger of PrP^C to PrP^β conversion and PrP amyloid fibril formation.[27−29] Thus, the amyloid fibril formation is sensitive to the pH environment. In this study, to obtain insight into the mechanism of pH-dependent structural conversion of preformed amyloid fibrils, pH-jump experiments were performed using H2 fibrils. We found that the conformation of H2 fibrils dramatically changed after the pH-jump from 2.9 to 7.5. Surprisingly, the fibril conformation nearly reverted after restoration of the solution pH to 2.9, as shown by CD and FT-IR spectra, and electron microscope (EM) observations. Moreover, kinetic analyses using the newly designed stopped-flow system adapted for amyloid fibrils revealed that these conformational changes can occur quite rapidly after the pH-jumps. Here we discuss these findings regarding the unique energy profile of H2 fibrils.

MATERIALS AND METHODS

H2 Peptide and Amyloid Fibril Formation. The amino acid sequence of the H2 peptide is QNNFVHDCVNITIKQHTVTTTTK, corresponding to a helix 2 of MoPrP (Figure S1 of the Supporting Information).[9] The H2 peptide was synthesized with Fmoc chemistry using a PS-3 peptide synthesizer (Protein Technologies, Tucson, AZ). The cleaved peptides was purified (>95%) by reversed phase HPLC using a COSMOSIL $5C_{18}$-AR-II column (Nacalai Tesque, Tyoto, Japan). The molecular weight of the peptide was measured by matrix-assisted laser desorption ionization time-of-flight (MALDI-TOF) mass spectrometry (Bruker Daltonics, Billerica, MA). H2 amyloid fibrils were formed using a peptide concentration of 100 μM (0.26 mg/mL) in 25 mM Gly−HCl buffer (pH 2.9) containing 100 mM NaCl at 37 °C without agitation. After 1 day of incubation, the conformation of the H2 fibrils was monitored by far-UV CD spectroscopy.

pH-Jump Experiments of H2 Amyloid Fibrils. In single pH-jump experiments from 2.9 to various pH values, the solution of H2 fibrils in 25 mM Gly−HCl (pH 2.9) containing 100 mM NaCl was diluted 2.5-fold with various pH solutions containing 25 mM buffers and 100 mM NaCl, and the solution pH was confirmed using a Handy pH Meter (Horiba, Kyoto, Japan). The following buffers were used: Gly−HCl (pH 1.9−

dx.doi.org/10.1021/bi400698u | Biochemistry 2013, 52, 6797−6806

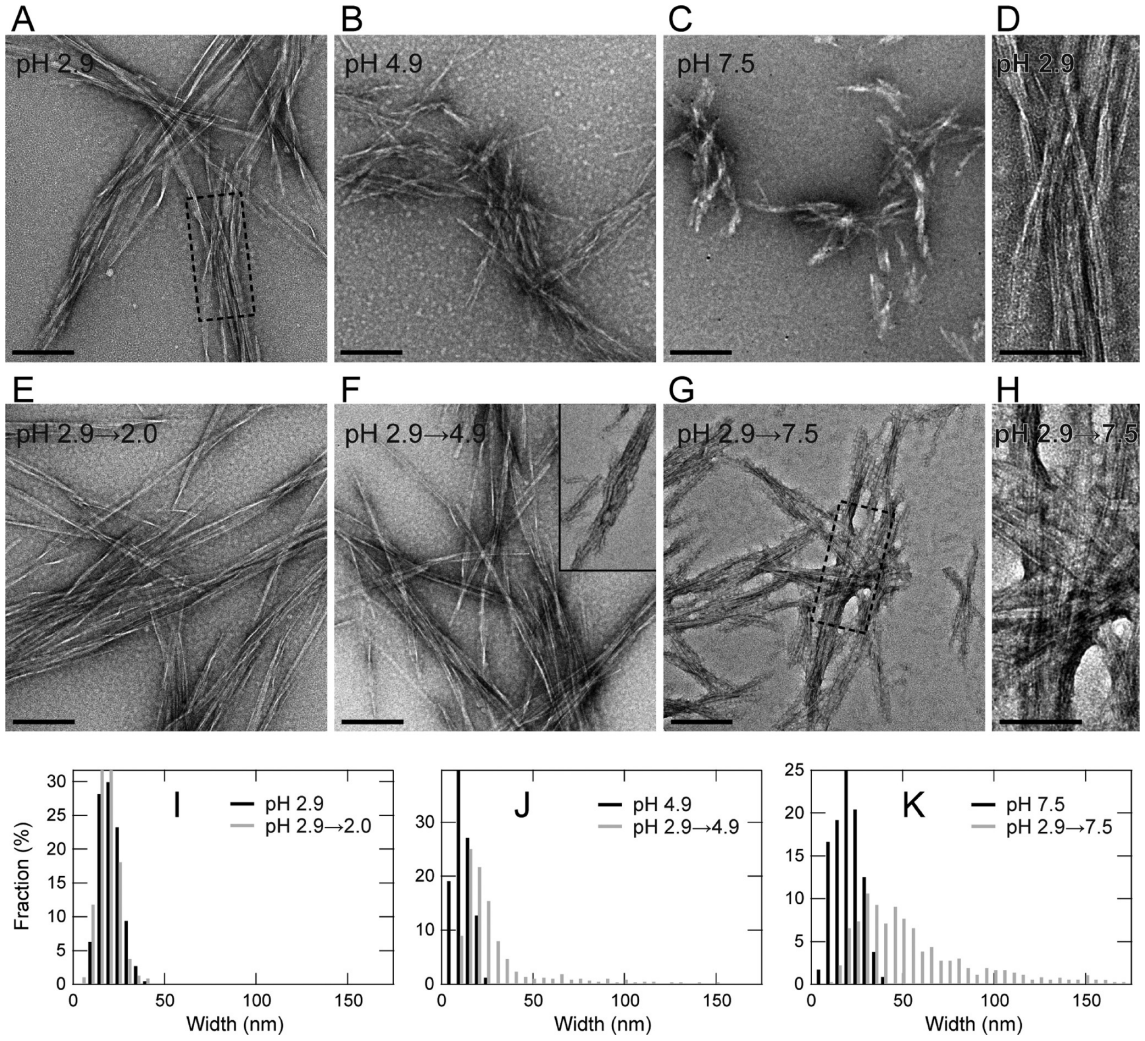

Figure 2. EM observations of H2 fibrils. (A)−(C) Amyloid fibrils prepared from the H2 peptide at pH 2.9 (A), 4.9 (B), and 7.5 (C) after 1 day of incubation. (E)−(G) H2 amyloid fibrils after the pH-jump from 2.9 to 2.0 (E), 4.9 (F), and 7.5 (G). The inset shows thick fibrils observed at other places after the pH-jump to 4.9. Scale bars = 200 nm. (D) and (H) Magnified images of H2 fibrils taken from panels (A) and (G), respectively. The magnified regions are indicated by the square. Scale bars = 100 nm. (I)−(K) Fibril width distribution of H2 fibrils formed at pH 2.9 (I, black bars), 4.9 (J, black bars), and 7.5 (K, black bars) before the pH-jump, and that of H2 fibrils after the pH-jump from 2.9 to 2.0 (I, gray bars), 4.9 (J, gray bars), and 7.5 (K, gray bars). Fibril widths of 230−410 fibrils were measured in each EM image, and the fraction (%) of each fibril width was plotted.

3.4), acetate−NaOH (pH 3.9−5.4), phosphate−NaOH (pH 5.9−7.0), Tris−HCl (pH 7.5−9.0), and Gly−NaOH (pH 9.5−10.1).

In double pH-jump experiments, first the H2 fibril solution at pH 2.9 was diluted 2.5-fold with 25 mM Tris−HCl containing 100 mM NaCl so that the solution pH was set to 7.5. After several times of incubation at 25 °C, the solution was diluted 2.5-fold again with 25 mM Gly−HCl containing 100 mM NaCl so that the solution pH was set to 2.9.

CD Measurement. Static far-UV CD spectra of H2 fibrils at various pH values were measured using a quartz cell with a light-path of 1 mm and a peptide concentration of 0.1 mg/mL at 25 °C on an AVIV model 215s spectropolarimeter (AVIV Biomedical, Lakewood, NJ). Kinetic far-UV CD spectra at 207 nm were measured at 25 °C after the pH-jumps, after manual mixing with a dead time of 30 s. The results are expressed as mean residue ellipticity $[\theta]$ (deg cm^2 dmol^{-1}).

EM Measurement. A 2-μL aliquot of sample solution was placed on a copper grid (400 mesh) covered with carbon film for 1 min, and excess solution was removed by blotting with filter paper. The grid was negatively stained with a 5-μL droplet of 2% uranyl acetate for 1 min. Again, the liquid on the grid was removed by blotting and dried. Electron micrographs were taken using a JEM-2100F transmission EM (JEOL, Tokyo, Japan), operating at 200 kV acceleration with a magnification of ×20,000.

Light Scattering Measurement and Precipitation Assay. Light scattering measurements of fibril solutions containing 0.05 mg/mL H2 fibrils, 25 mM buffers, and 100 mM NaCl at various pH values were performed with a Hitachi F-7000 fluorescence spectrophotometer at 25 °C. The wavelengths for excitation and emission were both set at 350 nm, and the slit length was 2.5 nm.

For precipitation assay, the solutions of H2 fibrils were centrifuged (30,000 × g at 4 °C for 1 h) to precipitate amyloid fibrils. The concentration of H2 peptide in supernatant was determined by UV absorption by applying the formula $(A_{215} - A_{225}) \times 144$ = protein concentration (μg/mL),[30] and the precipitated fraction was calculated by subtracting this value from the initial concentration of monomeric peptide.

dx.doi.org/10.1021/bi400698u | *Biochemistry* 2013, 52, 6797−6806

FT-IR Measurement. FT-IR absorption spectra were recorded with a Bruker Tensor 27 FT-IR spectrometer (Bruker Optics, Billerica, MA) equipped with a liquid N_2-cooled mercury cadmium telluride (MCT) detector and a BioATR II unit. The fibril solutions were centrifuged (30,000 × *g* at 4 °C for 1 h) to precipitate the fibrils, and the precipitated fibrils were loaded onto the surface of a BioATR II prism. The spectra were recorded at 25 °C with a resolution of 2 cm^{-1} and were averaged for 128 scans. From the spectrum of each sample, a corresponding buffer spectrum was subtracted. Difference spectra were calculated by subtracting the spectrum of absorption derived from C═O stretching of amide I, in which the range 1585−1715 cm^{-1} was corrected so as to be equal between two samples.

Development of Stopped-Flow Instrument and ANS Fluorescence Measurement. Kinetic ANS fluorescence data were collected by using a stopped-flow instrument manufactured in-house in order to flow amyloid fibril solution including large aggregates. The mixer possessing a Y-shaped channel with a diameter of 0.75 mm was connected using a PEEK tube with a diameter of 1.0 mm. A Hitachi F-7000 fluorescence spectrophotometer with a flow-cell set to a volume of 0.44 mL was used. The sample in the syringe was applied using a 200 V motor (Toshiba, Tokyo, Japan). The rotational frequency was regulated using a TOSVERT VF-nC3 inverter (Toshiba, Tokyo, Japan) to adjust the flow speed of the solution. NATA fluorescence measurements were performed at 25 °C with wavelengths of excitation at 295 nm and emission at 350 nm. The final concentration of NATA was kept constant at 1.8 μM after the 1:11.6 mixing of various concentrations of NBS and 2 μM NATA solutions. The mixing dead time was determined to be 130 ms by measuring the fluorescence quenching reaction of NATA by NBS. The refolding reaction of βLG was induced by dilution of urea from a concentration of 7.0 to 0.6 M at pH 3.0, and was monitored by the intensity change of Trp fluorescence with wavelengths of excitation at 295 nm and emission at 350 nm. The final concentration of βLG was 7.9 μM after the 1:11.6 mixing of denatured βLG solution and refolding buffer.

Static fluorescence measurements of 1-anilinonaphthalene-8-sulfonic acid (ANS) bound to the H2 fibrils were performed with excitation at 360 nm and monitored at 400−600 nm on a Hitachi F-7000 fluorescence spectrophotometer (Hitachi High-Tech, Tokyo, Japan). The fluorescence of the fibril solutions containing 0.01 mg/mL H2 fibrils, 25 mM buffers, 100 mM NaCl, and 10 μM ANS at various pH values was measured at 25 °C. ANS fluorescence spectrum in the absence of protein was used as baseline. Stopped-flow ANS fluorescence measurements to monitor the conformational changes of H2 fibrils were performed at 25 °C with wavelengths of excitation at 360 nm and emission at 475 nm. The final concentration of the H2 fibrils was 0.01 mg/mL after the 1:11.6 mixing of the fibril solution and pH-jump buffer, both of which contained 25 mM buffers, 100 mM NaCl, and 10 μM ANS. The following buffers were used: Gly−HCl (pH 2.9) and Tris−HCl (pH 7.5). The solution pH after mixing was confirmed using a Handy pH Meter. Nonlinear least-squares fitting was performed with IGOR Pro software (WaveMetrics, Lake Oswego, OR).

RESULTS

Single pH-Jump Experiments of H2 Amyloid Fibrils. As reported previously, at pH 2.9 the H2 peptide forms ordered amyloid fibrils with a minimum at 207 nm and immensely large negative ellipticity (−33,600 deg cm^2 $dmol^{-1}$) (Figure 1A, pH 2.9 fibrils), but at pH 7.5 it forms disordered fibrils with a minimum at 220 nm (−9900 deg cm^2 $dmol^{-1}$) (Figure 1A, pH 7.5 fibrils).[26] Although the CD spectrum of H2 fibrils at pH 2.9 has a minimum at 207 nm (Figure 1A), it is not α-helix conformation but corresponds to an ordered β-sheet conformation of H2 amyloid fibrils, because their FT-IR spectrum and second derivative show only intermolecular β-sheet and β-turn conformations, as described below (Figure 5A,D, pH 2.9 fibrils). In addition, the similar CD spectra have also been reported by other amyloid fibrils forming the ordered β-sheet conformation.[31,32] Moreover, since the CD spectra of model cyclic peptides, forming β-turn conformations of type I or II′, showed a minimum around 205 nm,[33−35] the CD spectrum of H2 fibrils at pH 2.9 would be a combination of β-sheet and type I or II′ β-turn conformations of ordered amyloid fibrils.[26] EM observations showed that relatively long and ordered fibrils, which consisted of several protofilaments, were formed at pH 2.9 (Figure 2A), while short and aggregate-like fibrils were formed at pH 7.5 (Figure 2C). Thus, the H2 peptide formed distinct types of fibrils depending on pH, and the formation of the long and ordered fibrils would be formed by the moderate repulsion between peptides. Here, we will refer to the fibrils formed at pH 2.9 as 'pH 2.9 fibrils', and those formed at pH 7.5 as 'pH 7.5 fibrils'.

Initially, we monitored various spectroscopic parameters associated with the structural conversion of preformed amyloid fibrils induced by pH-jumps from 2.9 to various pHs, 1.9−9.9. The pH was changed by diluting 2.5-fold with buffers containing the same concentration of salt. The CD spectra of pH 2.9 fibrils changed instantly with the pH (Figure 1A). Although the CD spectrum after the pH-jump to 3.9 was similar to that seen at pH 2.9, the ellipticity at 207 nm gradually decreased as the solution pH increased (Figure 1A,C), and the minimum shifted from 207 to 218 nm at the jump to pH 7.5 (Figure 1A). After the pH-jump to 7.5, the CD spectrum showed a minimum at 218 nm with relatively small ellipticity (−17,200 deg cm^2 $dmol^{-1}$) (Figure 1A), which somewhat resembled those for pH 7.5 fibrils formed without jump. Here, we named the fibrils formed after the jump to pH 7.5 'pH 7.5-like fibrils'. However, the CD ellipticities at 207 nm after pH-jumps to pH 6 to approximately 10 were negatively larger than those of fibrils formed at the same pH at equilibrium (Figure 1C). Thus, it appears that the pH 7.5-like fibrils partially retain the conformation of pH 2.9 fibrils, even after jumping to pH 7.5. After the pH-jump to pH 1.9, which is very acidic, ellipticity also decreased, but imperfectly returned to the level of fibrils formed at pH 1.9 at equilibrium (Figure 1A,C), suggesting hysteresis or large barriers between pH 2.9 fibrils and other fibrils formed at equilibrium.

Previously, we reported that two different types of amyloid fibrils are formed, depending on pH, and that the midpoint of the transition is approximately pH 5 (Figure 1C, □).[26] The midpoint of the conformational transition of fibrils following the pH jump also occurred at approximately pH 5 (Figure 1C, ○). Thus, the conformational changes of preformed H2 fibrils induced by the pH-jump were highly sensitive to the pH of the final solution, similar to the process of fibril formation from the monomeric peptide. Importantly, the conformational changes induced by manual pH-jumps from 2.9 to 4.5 or 7.5 were completed within the dead time of 30 s (Figure 1D), and these conformations were stable for at least 5 days (Figure 1D, inset). Since amyloid fibril formation of the H2 peptide requires at

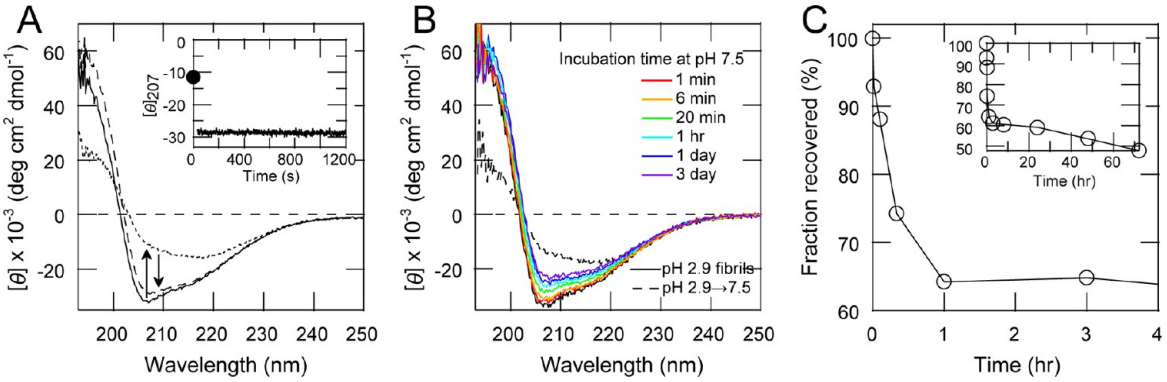

Figure 3. Conformational changes of H2 fibrils after the double pH-jump. (A) CD spectra of pH 2.9 fibrils before the pH-jump (solid line) and after a single pH-jump from 2.9 to 7.5 (dotted line), and a double pH-jump, pH 2.9 → 7.5 → 2.9 (dashed line). The inset shows the conformational changes of H2 fibrils after the double pH-jump, monitored as ellipticity at 207 nm. The ellipticity of H2 fibrils after the single pH-jump to 7.5 is shown by the closed circle. (B) CD spectra of H2 fibrils after incubation at pH 7.5 and 25 °C in the double pH-jump. The incubation times at pH 7.5 are depicted in the figure. CD spectra of H2 fibrils before the pH-jump at pH 2.9 (black solid line) and after the single pH-jump from 2.9 to 7.5 (black dashed line) are overlapped. (C) Incubation time-dependence at pH 7.5 in the double pH-jump experiment. The fraction recovered was estimated from the ellipticity at 207 nm. The inset shows the incubation time-dependence during 3 days of incubation.

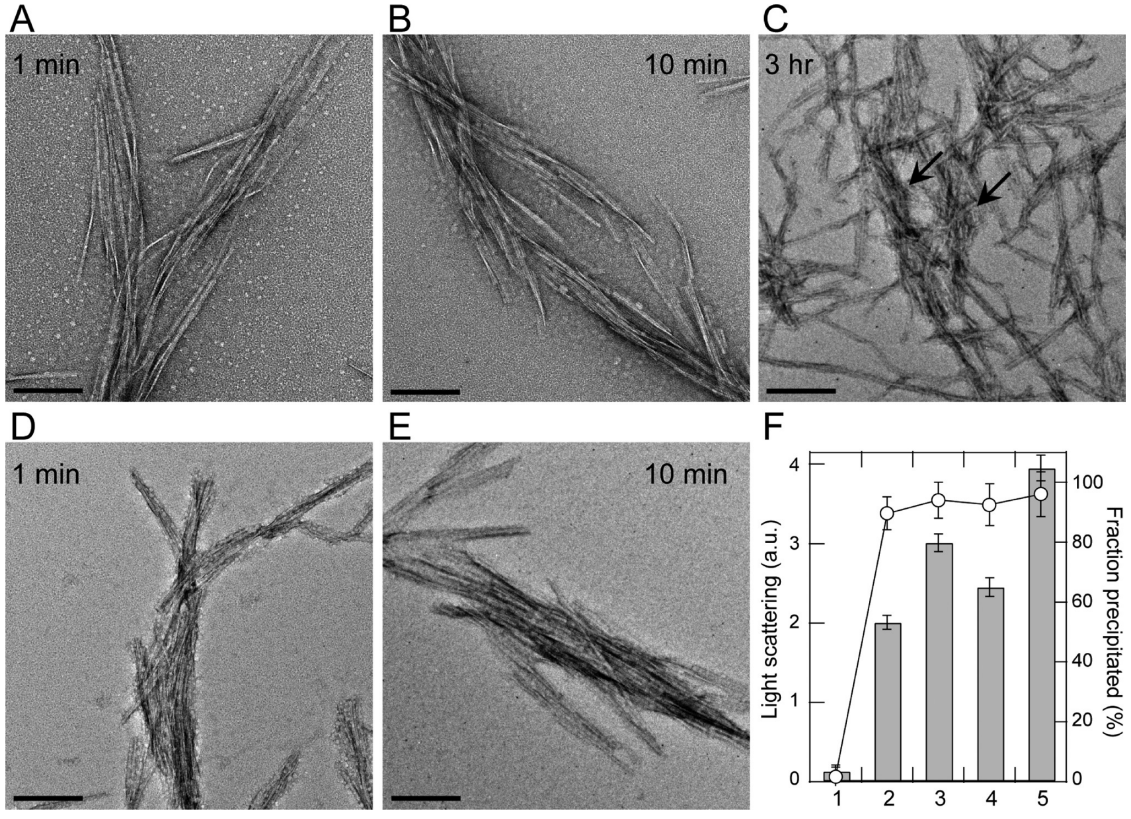

Figure 4. H2 amyloid fibrils after double pH-jump experiments. (A)−(E) EM images of H2 fibrils after incubation for 1 min (A,D), 10 min (B,E), and 3 h (C) at pH 7.5 and 25 °C in the double pH-jump. Thin fibrils (A,B) and thick fibrils (D,E), both types of fibrils (C) were observed. Thick fibrils are indicated by arrow (C). Scale bars are 200 nm. (F) Light scattering measurements (left ordinate, bar) and precipitated fraction (right ordinate, cycle) of H2 peptide monomer (1), and H2 fibrils before the pH-jump of pH 2.9 fibrils (2) and after a single pH-jump from 2.9 to 7.5 (3) and a double pH-jump pH 2.9 → 7.5 → 2.9 after incubation for 10 min at pH 7.5 (4), and pH 7.5 fibrils (5). The measurements were repeated three times.

least 3−4 h at 37 °C,[26] these conformational changes induced by the pH-jumps occurred directly, without involving the dissociation and subsequent aggregation process.

EM observations and fibril width distribution of H2 fibrils showed that after the pH-jump from 2.9 to 2.0, relatively long and thin amyloid fibrils with a diameter of 15−25 nm were observed (Figure 2E and I, gray), and their morphology and width were similar to those of pH 2.9 fibrils before the pH-jump (Figure 2A and I, black). After the pH-jump to 4.9, thin fibrils with a diameter of 15−20 nm (Figure 2F), which were ordered rather than those observed in the formation of fibrils from the monomer at pH 4.9 (Figure 2B), and a small number of thick fibrils were formed (Figure 2F, inset, and J, gray). After the pH-jump to 7.5, thick fibrils with a diameter of >50 nm

dx.doi.org/10.1021/bi400698u | *Biochemistry* 2013, 52, 6797−6806

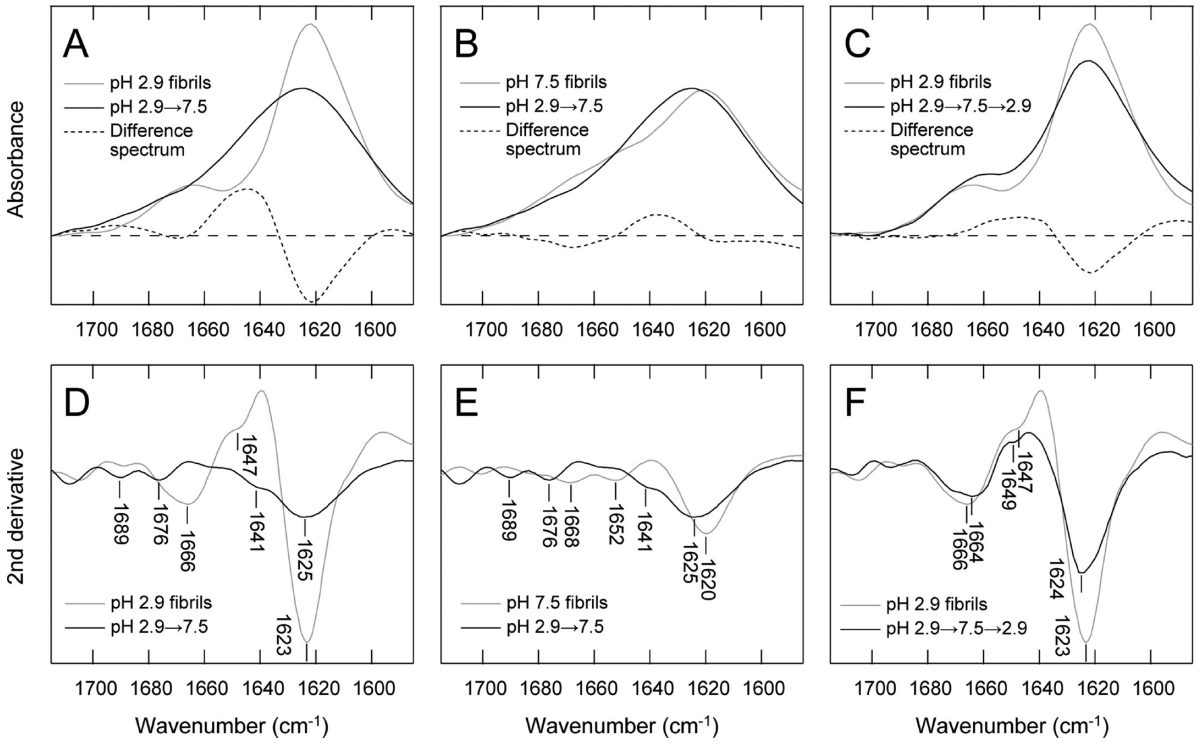

Figure 5. Conformation of H2 fibrils monitored by FT-IR spectra. (A)−(C) FT-IR absorption spectra of the fibrils before (gray solid line) and after (solid line) pH-jumps, and difference FT-IR spectra, subtracting the spectra before pH-jumps from those after pH-jumps (dotted line). (D)−(F) Secondary derivatives of FT-IR absorption spectra (A)−(C), respectively. Several β-sheet components are evident at 1620−1641 cm^{-1}, in addition to random conformations at 1647−1652 cm^{-1} and turn/loop conformations at 1664−1689 cm^{-1}.

(Figure 2K, gray), consisted of a large number of protofilaments, were observed (Figure 2G,H). Thus, pH 7.5-like fibrils (Figure 2K, gray) were much thicker than pH 2.9 fibrils before the pH-jump (Figure 2I, black). It is considered that the neutralization of electric repulsion between fibrils induces the assembly of fibrils. In fact, in the pH-jump to 7.5, the conformational change predominantly occurred along with the lateral association of the fibrils. Meanwhile, although the pH 2.9 fibrils consisted of several protofilaments (Figure 2A,D), the rotational symmetry axis[36] was unclear, and these fibrils often curved. The torsion of these fibrils was not recurrent. On the other hand, after the pH-jump from 2.9 to 7.5, protofilaments were fully assembled in pH 7.5-like fibrils (Figure 2H), but none of pH 2.9 fibrils and pH 7.5-like fibrils appears to associate with a rotational symmetry.

Double pH-Jump Experiments of H2 Amyloid Fibrils. The folding reaction of small-sized globular proteins is generally considered to be reversible at low protein concentrations.[37] Although a small number of reversible conformational or morphological changes of amyloid fibrils have been reported,[38,39] the mechanism of these reactions remains unknown. To investigate the reversibility of the conformational change of preformed H2 fibrils, a double pH-jump, pH 2.9 → 7.5 → 2.9, was performed using preformed by diluting 2.5-fold with buffers containing the same concentration of salt at every step. Intriguingly, pH 7.5-like fibrils with a minimum at 218 nm at pH 7.5 reverted to fibrils very similar to pH 2.9 fibrils, with an immensely large minimum at 207 nm at pH 2.9 (Figure 3A). These conformational changes were almost completed within the dead time of the manual pH-jump, 30 s (Figure 3A, inset). Next, the reversibility of pH 2.9 fibrils was investigated as a function of incubation time at pH 7.5. Efficiency gradually decreased as incubation time at pH 7.5 increased (Figure 3B,C). Although 93% of the pH 7.5-like fibrils reverted to pH 2.9 fibrils after 1 min of incubation at pH 7.5 (Figure 3C), after 72 h of incubation, approximately 50% of the pH 7.5-like fibrils had reverted to pH 2.9 fibrils. This irreversibility can be explained by the formation of an irreversible aggregate during the incubation at pH 7.5.

EM observations showed that, after the double pH-jump experiment with 1 min of incubation at pH 7.5, we observed two types of amyloid fibrils, one were thin fibrils (Figure 4A) and the other were thick fibrils consisted of a large number of protofilaments (Figure 4D). After 10 min of incubation at pH 7.5, we also observed thin (Figure 4B) and thick (Figure 4E) fibrils. After 3 h, we observed thin (Figure 4C) and thick (Figure 4C, arrow) fibrils. Although the population of these heterogeneous fibrils was unknown from EM measurements correctly, the fraction of fully recovered fibrils, which was obtained from CD measurements, decreased as the incubation time at pH 7.5 increased (Figure 3C).

Subsequently, light scattering measurements were performed to monitor the overall extent of fibril assembly (Figure 4F, left ordinate). After the pH-jump from 2.9 to 7.5 (Figure 4F, bar 3), the light-scattering intensity of pH 7.5-like fibrils increased to a level greater than that of pH 2.9 fibrils (Figure 4F, bar 2). After the double pH-jump, the light-scattering intensity of the fibrils slightly decreased (Figure 4F, bar 4), but remained larger than that before the pH-jump (Figure 4F, bar 2). These observations correspond to the EM observation that fibrils remained partially associated even after the double-pH jump (Figure 4C−E). In addition, all samples were centrifuged at 30,000 × g for 1 h, and the fractions of precipitated fibrils were estimated (Figure 4F, right ordinate). With the exception of H2 monomer (Figure 4F,

dx.doi.org/10.1021/bi400698u | Biochemistry 2013, 52, 6797−6806

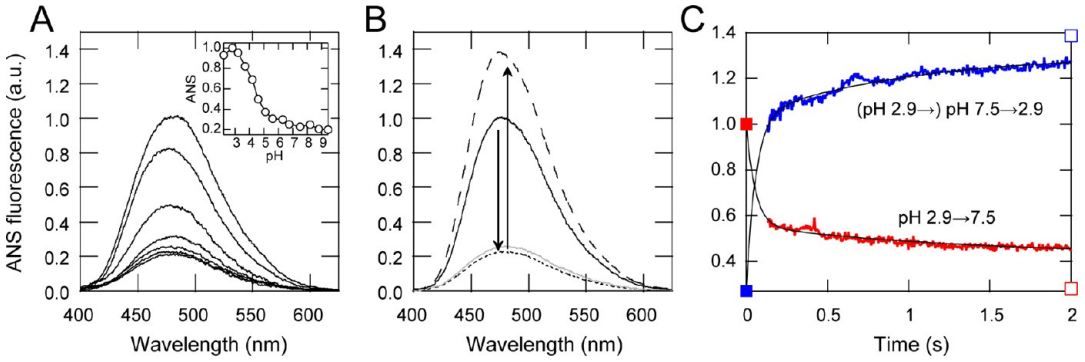

Figure 6. Conformational change of H2 fibrils monitored by ANS fluorescence stopped-flow. (A) Static ANS fluorescence spectra of the fibrils formed at various pHs. The solution pHs from top to bottom, at 475 nm are: pH 2.9, 3.7, 4.6, 5.6, 6.7, 7.5, and 8.8. The inset shows the ANS intensity at 475 nm as a function of pH. (B) H2 fibrils after a single pH-jump from 2.9 to 7.5 (dotted line) and a double pH-jump, pH 2.9 → 7.5 → 2.9, after incubation for 10 min at pH 7.5 (dashed line), and before the pH-jump of pH 2.9 fibrils (solid line) and pH 7.5 fibrils (gray solid line). (C) Kinetics of conformational changes of the H2 fibrils after a single pH-jump from 2.9 to 7.5 (red) and a double pH-jump, pH 2.9 → 7.5 → 2.9 (blue), after incubation for 10 min at pH 7.5. The intensities of the ANS fluorescence before and after the single pH-jump are shown by red closed and open squares, respectively, and before and after the double pH-jump are shown by blue closed and open squares, respectively.

circle 1), there was no large difference in the fractions of H2 fibrils (Figure 4F, circles 2−5). Thus, EM images roughly reflect the overall morphological features in the solutions.

Fibril Conformation Monitored by FT-IR Absorption Spectra. In order to characterize the secondary structure of H2 fibrils, FT-IR absorption spectra were measured in aqueous solution. The amide I band (1600−1700 cm^{-1}) is known to be a sensitive probe for determination of secondary structure.[40,41] The FT-IR spectrum of pH2.9 fibrils before the pH-jump revealed major bands corresponding to intermolecular β-sheet and β-turn conformations with bands at 1623 cm^{-1} and 1666 cm^{-1}, respectively (Figure 5A,D). After the pH-jump from 2.9 to 7.5, the FT-IR spectrum dramatically changed and showed an intermolecular β-sheet conformation with a band at 1625 cm^{-1}, and the band indicating a β-turn conformation was not seen at 1666 cm^{-1} but at 1676 and 1689 cm^{-1}, assigned to a turn/loop conformation (Figure 5A,D).[42] The difference spectrum showed an increase in random conformations, with a band at 1640−1655 cm^{-1}, and a decrease in intermolecular β-sheet conformations at around 1623 cm^{-1} (Figure 5A). Thus, it appears that the pH-jump causes the conformational change from pH 2.9 fibrils to pH 7.5-like fibrils by disrupting the highly ordered β-sheet and β-turn conformations, coupled with a decrease in CD ellipticity at 207 nm (Figure 1A).

The FT-IR spectrum of the pH 7.5-like fibrils was certainly distinct from that of the pH 7.5 fibrils formed at pH 7.5 (Figure 5B,E). The difference spectrum showed that pH 7.5-like fibrils were somewhat rich in β-sheet conformation, with a band at 1630−1640 cm^{-1}, and poor in turn/loop conformation, with band at approximately 1668 cm^{-1} (Figure 5B). It appears that the β-sheet hydrogen bonds of pH 2.9 fibrils remain partially intact even after the pH-jump to 7.5, which leads to the large negative CD ellipticity, unlike that of fibrils formed at pH 7.5 (Figure 1A).

After the double pH-jump, pH 2.9 → 7.5 → 2.9, the major bands corresponding to intermolecular β-sheet and β-turn conformations, with bands at 1624 cm^{-1} and 1664 cm^{-1}, respectively, are comparable with the bands of pH 2.9 fibrils before the pH-jump (Figure 5C,F). However, the difference spectrum showed a decrease in intermolecular β-sheet conformations and an increase in random conformations at approximately 1624 cm^{-1} and 1649 cm^{-1} (Figure 5C), respectively. This result suggests that although the pH 7.5-like fibrils revert to a conformation very similar to that of the pH 2.9 fibrils, even after the double pH-jump they are contaminated with some fraction of the pH 7.5-like fibrils, as shown by the EM observations (Figure 4C−E).

Kinetic Analyses of Conformational Changes of H2 Fibrils Using ANS Fluorescence Stopped-Flow. To monitor the conformational changes of H2 fibrils within the dead time of manual mixing, a stopped-flow instrument composed of a PEEK tube with a diameter of 1.0 mm and a Y-shaped mixer with a 0.75-mm-diameter channel was manufactured. The instrument was designed to create laminar flow and efficient mixing of the amyloid fibril solution, including large aggregates, without choking. First, the dead time of the stopped-flow was estimated using the quenching reaction of *N*-acetyl-L-tryptophane-amide (NATA) fluorescence by *N*-bromosuccinimide (NBS) (Figure S2 of the Supporting Information),[43,44] and a dead time of 130 ms was obtained. In addition, the refolding reaction of β-lactoglobulin (βLG) was examined using Trp fluorescence (Figure S3 of the Supporting Information). The end of a transient overshoot corresponding to the partially structured intermediate populated on the millisecond time scale[45] was observed.

Subsequently, the conformation of H2 fibrils formed at various pH values was examined using static fluorescence of 1-anilinonaphthalene-8-sulfonic acid (ANS). The fluorescence intensity of ANS bound to the fibrils gradually decreased as the pH value of the solution increased (Figure 6A), indicating that the hydrophobic region that is partially exposed to the solvent in the aggregate-like fibrils formed around neutral pH is smaller than that in the thin fibrils formed at acidic pHs. It appears that in aggregate-like fibrils the hydrophobic region is buried within the associated fibrils (Figure 2C).

Next, the conformational change of H2 fibrils induced by the pH-jump from 2.9 to 7.5 was examined. The ANS fluorescence dramatically decreased to a level similar to that of aggregate-like pH 7.5 fibrils (Figure 6B), following the conformational change from pH 2.9 fibrils to pH 7.5-like fibrils. After the double pH-jump, pH 2.9 → 7.5 → 2.9, the ANS fluorescence increased by 1.4-fold over that observed in the pH2.9 fibrils before the pH-jump (Figure 6B). Although the precise details are unknown, it appears that the H2 fibrils may partially disorder after the double pH-jump, exposing the much more hydrophobic domains to the solvent. However, the CD and FT-IR spectra

dx.doi.org/10.1021/bi400698u | *Biochemistry* 2013, 52, 6797−6806

and EM observations showed that the conformation of pH 2.9 fibrils reverted almost completely, as described above. Then, the kinetic conformational changes of the H2 fibrils were examined by combining ANS fluorescence and stopped-flow. After the single pH-jump from 2.9 to 7.5, the conformational change of the fibrils was instantaneous and could not be monitored within the dead time of 130 ms (Figure 6C). We analyzed the experimental data according to the following kinetic formula:

$$f(t) = A_0 + A_1\exp(-k_1 t) + A_2\exp(-k_2 t) \quad (1)$$

Although its trace could not be completely fitted by a double exponential curve (eq 1), it appears that the apparent rate constant of the fast phase (k_1), which may consist of several phases, was larger than 18.3 ± 1.01 s^{-1} and that of slow phase (k_2) was 0.73 ± 0.03 s^{-1}. After restoration of the solution pH to 2.9, the conformation of the fibrils again changed readily (Figure 6C). The fluorescence intensity was fitted by a double exponential curve relatively well, and the apparent rate constants of the fast (k_{-1}) and slow (k_{-2}) phases, after the double pH-jump, were determined to be 17.6 ± 0.77 s^{-1} and 1.05 ± 0.04 s^{-1}, respectively. Intriguingly, the kinetic constants of the fast and slow phases were almost identical between the single and the double pH-jumps, implying similar conversion processes of the fibrils, such as lateral association or dissociation of the preformed fibrils. Collectively, amyloid fibrils can be readily and nearly reversibly converted between two distinct conformations separated by a low energy barrier.

DISCUSSION

Amyloidogenicity of Helix 2 Region of PrP. Recent studies indicate that the low pH solution is an ideal trigger of PrP^C to PrP^β conversion and PrP amyloid fibril formation.[27−29] The salt bridges of native PrP have been calculated and analyzed by quantum chemical calculations,[46] and the detailed biophysical characteristics and NMR studies of $PrP^C \rightarrow PrP^\beta$ conversion process have also been reported.[28] Recently, incorporating Wenxiang diagrams[29,47,48] further summarized their research based on the NMR, CD spectra, and dynamic light scattering data at the low pH environment found that some salt bridges and the hydrophobic interactions in the three helices of the prion proteins can affect the helical structural stability. These studies have provided insight into the prion misfolding and the mechanism of amyloid fibril formation. According to the experimental results[49,50] and recent Wenxiang diagram analysis,[29] the helical structure of H1 is much more stable than that of helices H2 and H3, and helix H3 is more stable than H2.[29,46] Therefore, unstable H2 helix should be more easily converted to H2 fibrils under acidic pH environment. In addition, after the disulfide bond of PrP is reduced, helix H2 is no longer stable and is partially unfolded in the PrP structural conversion.[51] This is why H2 peptide is selected to study the pH-jump induced conformational transition.

Conformation Change of H2 Fibrils was Induced by a Single pH-Jump. In general, it is considered that amyloid fibrils, which are highly ordered supramolecular complexes, are stiffer than most functional intracellular biological filaments,[21] and are rigid like a needle. X-ray microcrystallography has revealed that the amyloid fibrils are composed of a pair of β-sheets with the facing side chains interdigitated in a steric zipper and are extremely highly ordered.[20,52] However, after pH-jump from 2.9 to 7.5, H2 fibril conformation readily changed to a distinct one as revealed by CD and FT-IR spectra (Figures 1 and 5), and morphological conversion from thin pH 2.9 fibrils to thick pH 7.5-like fibrils occurred (Figure 2D,H). Recently, Kurouski et al. reported the pH-induced conformational changes in insulin fibrils were detected using vibrational circular dichroism and fluid-cell atomic force microscope,[16] and temperature-induced structural rearrangement has also been reported for MoPrP fibrils.[38]

In the high pressure experiment, amyloid fibrils of β_2-microglobulin showed the structural reorganization into more tightly packed ones,[53] implying that amyloid fibrils are not tightly packed and contain a large number of cavities at atmosphere. Thus, although amyloid fibrils seem to be rigid, mature amyloid fibrils may not represent the most thermodynamically stable state.[16,38,53] Amyloid fibrils are proposed to be determined predominantly by the hydrogen bond network in the extended intermolecular β-sheet architecture of the peptide backbones,[21] but the packing between the side-chains may not be optimized.[16,38,53] Hence, it is possible that interactions between the side-chains modulate fibril conformation when the pH of the solution changes. In addition, these conversions were completed within a few seconds (Figure 6C). The pH profile of the conversions was almost identical to that of fibril formation for the H2 peptide (Figure 1C), both of which significantly changed at approximately pH 5. Thus, it appears that the side-chains of the H2 peptide were substantially exposed to the solvent when the fibrils were formed, enabling the rapid conformational change of the fibrils.

Nearly Reversible Conformational Change of H2 Fibrils After a Double pH-Jump. Intriguingly, the conformation of pH 7.5-like fibrils reverted to a conformation very similar to that of pH 2.9 fibrils when the solution pH was restored from 7.5 to 2.9 (Figure 3A), and these conversions were completed rapidly (Figure 6C). EM observation showed that the thick laterally associated pH 7.5-like fibrils dissociated into the thin pH 2.9 fibrils (Figure 4A,B), induced by electric repulsion between fibrils that were stacked by hydrophobic interactions at pH 7.5. Notably, these phenomena may be particular to amyloid fibrils and may not be observed for random aggregates, and observation of these results will depend on partial maintenance of the conformation of pH 2.9 fibrils after the pH-jump to 7.5. The CD and FT-IR spectra showed that pH 7.5-like fibrils, prepared by the pH-jump from 2.9 to 7.5, were certainly distinct from fibrils formed at pH 7.5 (Figures 1A and 5E).

In general, globular monomeric proteins readily relax conformation depending on the conditions, but amyloid fibrils are supramolecular complexes whose global conformational changes may be hindered by hydrogen bonds and hydrophobic interactions between both sides of the molecules, unless the fibrils dissolve into monomers. The partial remaining hydrogen bond network in the intermolecular β-sheet of the backbones, which may act like a clasp, can allow rapid reversible conformational changes between pH 7.5 and 2.9 by decreasing the energy of transition between pH 7.5-like fibrils and pH 2.9 fibrils. Thus, its rate constant was comparable to that of globular monomer protein folding.[54,55] If the pattern of hydrogen bonds were completely altered by the pH-jump, more time would be required to return to either the initial conformation or the distinct conformation of amyloid fibrils. In contrast, the reversibility decreased as incubation time at pH 7.5 increased (Figure 3C), because the amyloid fibrils could

dx.doi.org/10.1021/bi400698u | Biochemistry 2013, 52, 6797−6806

gradually become strongly associated with each other through hydrophobic interactions. Thus, conformational change of the fibrils is feasible before they form large aggregates.

Proposed Pathways of Conformational Changes of H2 Fibrils. The H2 peptide formed pH 2.9 fibrils and pH 7.5 fibrils at pH 2.9 and 7.5, respectively (Figure 7). Their

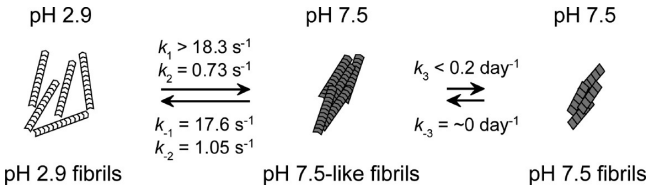

Figure 7. Proposed pathways of conformational changes of H2 fibrils. The H2 peptide formed pH 2.9 fibrils (left) and pH 7.5 fibrils (right) at pH 2.9 and 7.5, respectively. After the pH-jump from 2.9 to 7.5, pH 2.9 fibrils instantly changed to pH 7.5-like fibrils (middle), and reverted to pH 2.9 fibrils when the solution pH was restored to 2.9. The thick, laterally associated fibrils (middle) or aggregated fibrils (right) stacked by the hydrophobic interactions at pH 7.5 were painted gray.

conformations and morphologies are significantly different. After the pH-jump from 2.9 to 7.5, pH 2.9 fibrils instantly changed to pH 7.5-like fibrils, but pH 7.5-like fibrils partially retained the intermolecular hydrogen bonds of pH 2.9 fibrils. In addition, pH 7.5-like fibrils reverted to pH 2.9 fibrils when the solution pH was restored to 2.9 (Figure 7). Thus, the transition energy between pH 2.9 fibrils and pH 7.5-like fibrils is relatively low, and the relatively fast phases in the conversion between them were observed (0.7−18 s^{-1}). In contrast, the pH 7.5-like fibrils did not change to the pH 7.5 fibrils for at least 5 days (Figure 1D, inset), and pH 7.5 fibrils also did not change to pH 7.5-like fibrils even under identical conditions (data not shown), suggesting the presence of a high energy barrier between them (<0.2 day^{-1}) (Figure 7). To exceed these energy barriers, it might be necessary to break down the intermolecular restrictions in these fibrils completely.

These conformational changes of H2 fibrils were caused by the disruption of the balance between hydrophobic and electrostatic interactions resulting from the change in the solution pH, and thus the amyloid fibrils may have the potential to convert into distinct forms depending on the conditions. Theses conformational varieties of the amyloid fibrils may explain the physical background of the diversity in prion.

■ ASSOCIATED CONTENT

Supporting Information

Structure of MoPrP(121−231) and amino acid sequence of H2 peptide (MoPrP(172−194)), estimation of the dead-time of the stopped-flow instrument, and refolding of β-lactoglobulin (βLG) from the urea-denatured state at pH 3.0. This material is available free of charge via the Internet at http://pubs.acs.org.

■ AUTHOR INFORMATION

Corresponding Author

*Phone: +81 58 230 6145. E-mail: kuwata@gifu-u.ac.jp.

Funding

This work was supported by the Program for the Promotion of Fundamental Studies in Health Science of the National Institute of Biomedical Innovation, and by a grant from Research on Measures for Intractable Diseases (Prion Disease and Slow Virus Infections) of the Ministry of Health, Labour and Welfare of Japan. K. Yamaguchi was supported by the Japan Society for Promotion of Science (JSPS) Research Fellowship for Young Scientists. Y. O. Kamatari and K. Kuwata were supported by Grants-in-Aid for Scientific Research and X-ray Free Electron Laser (XFEL) program of the Ministry of Education, Culture, Sports, Science and Technology of Japan.

Notes

The authors declare no competing financial interest.

■ ACKNOWLEDGMENTS

We thank the Equipment Center for Common Research at the Graduate School of Medicine, Gifu University, for assistance with EM observations.

■ ABBREVIATIONS

ANS, 1-anilinonaphthalene-8-sulfonic acid; CD, circular dichroism; EM, electron microscope; FT-IR, Fourier transform infrared; H2 peptide, fragmented peptide of helix 2; MoPrP, mouse prion protein; PrP^{C}, cellular form of prion protein; PrP^{Sc}, scrapie form of prion protein; ThT, thioflavin T

■ REFERENCES

(1) Rochet, J. C., and Lansbury, P. T., Jr. (2000) Amyloid fibrillogenesis: themes and variations. *Curr. Opin. Struct. Biol. 10*, 60−68.

(2) Cohen, F. E., and Kelly, J. W. (2003) Therapeutic approaches to protein-misfolding diseases. *Nature 426*, 905−909.

(3) Prusiner, S. B. (1998) Prions. *Proc. Natl. Acad. Sci. U.S.A. 95*, 13363−13383.

(4) Uversky, V. N., and Fink, A. L. (2004) Conformational constraints for amyloid fibrillation: the importance of being unfolded. *Biochim. Biophys. Acta 1698*, 131−153.

(5) Collinge, J., Sidle, K. C. L., Meads, J., Ironside, J., and Hill, A. F. (1996) Molecular analysis of prion strain variation and the aetiology of 'new variant' CJD. *Nature 383*, 685−690.

(6) Bruce, M. E., Will, R. G., Ironside, J. W., McConnell, I., Drummond, D., Suttie, A., McCardle, L., Chree, A., Hope, J., Birkett, C., Cousens, S., Fraser, H., and Bostock, C. J. (1997) Transmissions to mice indicate that 'new variant' CJD is caused by the BSE agent. *Nature 389*, 498−501.

(7) Aguzzi, A., and Polymenidou, M. (2004) Mammalian prion biology: one century of evolving concepts. *Cell 116*, 313−327.

(8) Weissmann, C. (2004) The state of the prion. *Nat. Rev. Microbiol. 2*, 861−871.

(9) Riek, R., Hornemann, S., Wider, G., Billeter, M., Glockshuber, R., and Wuthrich, K. (1996) NMR structure of the mouse prion protein domain PrP(121−231). *Nature 382*, 180−182.

(10) Pan, K.-M., Baldwin, M., Nguyen, J., Gasset, M., Serban, A., Groth, D., Mehlhorn, I., Huang, Z., Fletterick, R. J., Cohen, F. E., and Prusiner, S. B. (1993) Conversion of α-helices into β-sheets features in the formation of the scrapie prion proteins. *Proc. Natl. Acad. Sci. U.S.A. 90*, 10962−10966.

(11) Collinge, J. (2001) Prion diseases of humans and animals: their causes and molecular basis. *Annu. Rev. Neurosci. 24*, 519−550.

(12) Jones, E. M., and Surewicz, W. K. (2005) Fibril conformation as the basis of species-and strain-dependent seeding specificity of mammalian prion amyloids. *Cell 121*, 63−72.

(13) Makarava, N., Ostapchenko, V. G., Savtchenko, R., and Baskakov, I. V. (2009) Conformational switching within individual amyloid fibrils. *J. Biol. Chem. 284*, 14386−14395.

(14) Ban, T., Yamaguchi, K., and Goto, Y. (2006) Direct observation of amyloid fibril growth, propagation, and adaptation. *Acc. Chem. Res. 39*, 663−670.

(15) Li, J., Browning, S., Mahal, S. P., Oelschlegel, A. M., and Weissmann, C. (2010) Darwinian evolution of prions in cell culture. *Science 327*, 869−872.
(16) Kurouski, D., Dukor, R. K., Lu, X., Nafie, L. A., and Lednev, I. K. (2012) Spontaneous inter-conversion of insulin fibril chirality. *Chem. Commun. 48*, 2837−2839.
(17) Van Melckebeke, H., Wasmer, C., Lange, A., Ab, E., Loquet, A., Böckmann, A., and Meier, B. H. (2010) Atomic-resolution three-dimensional structure of HET-s(218−289) amyloid fibrils by solid-state NMR spectroscopy. *J. Am. Chem. Soc. 132*, 13765−13775.
(18) Paravastu, A. K., Leapman, R. D., Yau, W.-M., and Tycko, R. (2008) Molecular structural basis for polymorphism in Alzheimer's β-amyloid fibrils. *Proc. Natl. Acad. Sci. U.S.A. 105*, 18349−18354.
(19) Iwata, K., Fujiwara, T., Matsuki, Y., Akutsu, H., Takahashi, S., Naiki, H., and Goto, Y. (2006) 3D structure of amyloid protofilaments of β_2-microglobulin fragment probed by solid-state NMR. *Proc. Natl. Acad. Sci. U.S.A. 103*, 18119−18124.
(20) Sawaya, M. R., Sambashivan, S., Nelson, R., Ivanova, M. I., Sievers, S. A., Apostol, M., Thompson, M. J., Balbirnie, M., Wiltzius, J. J. W., McFarlane, H. T., Madsen, A., Riekel, C., and Eisenberg, D. (2007) Atomic structures of amyloid cross-β spines reveal varied steric zippers. *Nature 447*, 453−457.
(21) Knowles, T. P., Fitzpatrick, A. W., Meehan, S., Mott, H. R., Vendruscolo, M., Dobson, C. M., and Welland, M. E. (2007) Role of intermolecular forces in defining material properties of protein nanofibrils. *Science 318*, 1900−1903.
(22) Kaylor, J., Bodner, N., Edridge, S., Yamin, G., Hong, D.-P., and Fink, A. L. (2005) Characterization of oligomeric intermediates in α-synuclein fibrillation: FRET studies of Y125W/Y133F/Y136F α-synuclein. *J. Mol. Biol. 353*, 357−372.
(23) Bitan, G., Kirkitadze, M. D., Lomakin, A., Vollers, S. S., Benedek, G. B., and Teplow, D. B. (2003) Amyloid β-protein (Aβ) assembly: Aβ40 and Aβ42 oligomerize through distinct pathways. *Proc. Natl. Acad. Sci. U.S.A. 100*, 330−335.
(24) Kyte, J., and Doolittle, R. F. (1982) A simple method for displaying the hydropathic character of a protein. *J. Mol. Biol. 157*, 105−132.
(25) Deléage, G., Combet, C., Blanchet, C., and Geourjon, C. (2001) ANTHEPROT: an integrated protein sequence analysis software with client/server capabilities. *Comput. Biol. Med. 31*, 259−267.
(26) Yamaguchi, K., Matsumoto, T., and Kuwata, K. (2008) Critical region for amyloid fibril formation of mouse prion protein: unusual amyloidgenic properties of the helix 2 peptide. *Biochemistry 47*, 13242−13251.
(27) Gerber, R., Tahiri-Alaoui, A., Hore, P. J., and James, W. (2008) Conformational pH dependence of intermediate states during oligomerization of the human prion protein. *Protein Sci. 17*, 537−544.
(28) Bjorndahl, T. C., Zhou, G. P., Liu, X., Perez-Pineiro, R., Semenchenko, V., Saleem, F., Acharya, S., Bujold, A., Sobsey, C. A., and Wishart, D. S. (2011) Detailed biophysical characterization of the acid-induced PrP(c) to PrP(β) conversion process. *Biochemistry 50*, 1162−1173.
(29) Zhou, G. P., and Huang, R. B. (2013) The pH-triggered conversion of the PrP^{C} to PrP^{Sc}. *Curr. Top. Med. Chem. 13*, 1152−1163.
(30) Weddell, W. J. (1956) A simple ultraviolet spectrophotometric method for the determination of protein. *J. Lab. Clin. Med. 48*, 311−314.
(31) Adachi, R., Yamaguchi, K., Yagi, H., Sakurai, K., Naiki, H., and Goto, Y. (2007) Flow-induced alignment of amyloid protofilaments revealed by linear dichroism. *J. Biol. Chem. 282*, 8978−8983.
(32) Saiki, M., Honda, S., Kawasaki, K., Zhou, D., Kaito, A., Konakahara, T., and Morii, H. (2005) Higher-order molecular packing in amyloid-like fibrils constructed with linear arrangements of hydrophobic and hydrogen-bonding site-chains. *J. Mol. Biol. 348*, 983−998.
(33) Hollósi, M., Kövér, K. E., Holly, S., Radics, L., and Fasman, G. D. (1987) β-Turns in bridged proline-containing cyclic peptide models. *Biopolymers 26*, 1555−1572.
(34) Gierasch, L. M., Deber, C. M., Madison, V., Niu, C. H., and Blout, E. R. (1981) Conformations of $(X\text{-}_{L}\text{-Pro-Y})_2$ cyclic hexapeptides. Preferred β-turn conformers and implications for β-turns in proteins. *Biochemistry 20*, 4730−4738.
(35) Rose, G. D., Gierasch, L. M., and Smith, J. A. (1985) Turns in peptides and proteins. *Adv. Protein Chem. 37*, 1−109.
(36) Fujii, T., Iwane, A. H., Yanagida, T., and Namba, K. (2010) Direct visualization of secondary structures of F-actin by electron cryomicroscopy. *Nature 467*, 724−728.
(37) Anfinsen, C. B. (1973) Principles that govern the folding of protein chains. *Science 181*, 223−230.
(38) Bocharova, O. V., Makarava, N., Breydo, L., Anderson, M., Salnikov, V. V., and Baskakov, I. V. (2006) Annealing prion protein amyloid fibrils at high temperature results in extension of a proteinase K-resistant core. *J. Biol. Chem. 281*, 2373−2379.
(39) Sabaté, R., Baxa, U., Benkemoun, L., Sánchez de Groot, N., Coulary-Salin, B., Maddelein, M. I., Malato, L., Ventura, S., Steven, A. C., and Saupe, S. J. (2007) Prion and non-prion amyloids of the HET-s prion forming domain. *J. Mol. Biol. 370*, 768−783.
(40) Barth, A., and Zscherp, C. (2002) What vibrations tell us about proteins. *Q. Rev. Biophys. 35*, 369−430.
(41) Seshadri, S., Khurana, R., and Fink, A. L. (1999) Fourier transform infrared spectroscopy in analysis of protein deposits. *Methods Enzymol. 309*, 559−576.
(42) Bandekar, J. (1992) Amide modes and protein conformation. *Biochim. Biophys. Acta 1120*, 123−143.
(43) Bilsel, O., Kayatekin, C., Wallace, L. A., and Matthews, C. R. (2005) A microchannel solution mixer for studying microsecond protein folding reactions. *Rev. Sci. Instrum. 76*, 014302.
(44) Peterman, B. F. (1979) Measurement of the dead time of a fluorescence stopped-flow instrument. *Anal. Biochem. 93*, 442−444.
(45) Kuwata, K., Shastry, R., Cheng, H., Hoshino, M., Batt, C. A., Goto, Y., and Roder, H. (2001) Structural and kinetic characterization of early folding events in β-lactoglobulin. *Nat. Struct. Biol. 8*, 151−155.
(46) Ishikawa, T., and Kuwata, K. (2010) Interaction analysis of the native structure of prion protein with quantum chemical calculations. *J. Chem. Theor. Comput. 6*, 538−547.
(47) Chou, K. C., Zhang, C. T., and Maggiora, G. M. (1997) Disposition of amphiphilic helices in heteropolar environments. *Proteins 28*, 99−108.
(48) Chou, K. C., Lin, W. Z., and Xiao, X. (2011) Wenxiang: a web-server for drawing wenxiang diagrams. *Nat. Sci. 3*, 862−865.
(49) DeMarco, M. L., and Daggett, V. (2007) Molecular mechanism for low pH triggered misfolding of the human prion protein. *Biochemistry 46*, 3045−3054.
(50) Ziegler, J., Sticht, H., Marx, U. C., Müller, W., Rösch, P., and Schwarzinger, S. (2003) CD and NMR studies of prion protein (PrP) helix 1. Novel implications for its role in the $PrP^{C}\rightarrow PrP^{Sc}$ conversion process. *J. Biol. Chem. 278*, 50175−50181.
(51) Sang, J. C., Lee, C.-Y., Luh, F. Y., Huang, Y.-W., Chiang, Y.-W., and Chen, R. P. (2012) Slow spontaneous α-to-β structural conversion in a non-denaturing neutral condition reveals the intrinsically disordered property of the disulfide-reduced recombinant mouse prion protein. *Prion 6*, 489−497.
(52) Nelson, R., Sawaya, M. R., Balbirnie, M., Madsen, A. Ø., Riekel, C., Grothe, R., and Eisenberg, D. (2005) Structure of the cross-β spine of amyloid-like fibrils. *Nature 435*, 773−778.
(53) Chatani, E., Kato, M., Kawai, T., Naiki, H., and Goto, Y. (2005) Main-chain dominated amyloid structures demonstrated by the effect of high pressure. *J. Mol. Biol. 352*, 941−951.
(54) Baker, D. (2000) A surprising simplicity to protein folding. *Nature 405*, 39−42.
(55) Kamagata, K., Arai, M., and Kuwajima, K. (2004) Unification of the folding mechanisms of non-two-state and two-state proteins. *J. Mol. Biol. 339*, 951−965.